Combined Heat Transfer and Fluid Dynamic Measurements Downstream of a Backward-Facing Step

J. C. Vogel[1]
Research Assistant.

J. K. Eaton
Assistant Professor.
Mem. ASME

Mechanical Engineering Department,
Stanford University,
Stanford, CA 94305

Combined heat transfer and fluid dynamic measurements in a separated and reattaching boundary layer, with emphasis on the near-wall region, are presented. A constant heat-flux surface behind a single-sided sudden expansion is used to obtain Stanton number profiles as a function of Reynolds number and boundary-layer thickness at separation. Fluctuating skin-friction and temperature profiles demonstrate the importance of the near-wall region in controlling the heat transfer rate. The fluctuating skin friction controls the heat transfer rate near reattachment, while the conventional Reynolds analogy applies in the redeveloping boundary layer beginning two or three step heights downstream of reattachment.

Introduction

In many flows of practical interest, separation of a boundary layer and subsequent reattachment of the separated layer to a solid surface is unavoidable. Such flows occur in nuclear reactors, gas turbines, electronic circuitry, and heat transfer devices. Reattaching flows are a serious problem for the heat transfer engineer, because they can cause large variations of the local heat transfer coefficient as well as substantial overall heat transfer augmentation. A design method is needed to predict thermal loads caused by reattachment.

When a predictive design method is developed, it will most probably be based on computational fluid mechanics. Several calculation techniques have been developed which can adequately reproduce the gross fluid mechanical features of separated flow fields (see the detailed review of the results of 18 methods in Eaton [1]). Efforts are now under way to extend the models to predict heat transfer. Experimental work is needed to gain a physical understanding of the flow and to provide detailed information for comparison with models.

Most of the previous work on reattachment involved study of the hydrodynamics of backward-facing step flows. Eaton and Johnston [2] and Watkins and Gooray [3] reviewed the literature in this area. A large number of early studies served to delineate the basic characteristics of reattaching flows, but could not provide quantitative data. More recently, experimenters have used the pulsed-wire anemometer (e.g., Eaton and Johnston [4]) and the laser-doppler anemometer (LDA) (e.g., Durst and Tropea [5]) to supply quantitative data in the highly turbulent reattaching flow. Near-wall velocity data have only recently become available with the advent of the thermal tuft (Eaton et al. [6]), the pulsed wall probe (Westphal et al. [7]), and specially configured LDA systems.

There have been fewer studies of heat transfer in reattaching flows. Fletcher et al. [8], Aung and Watkins [9], and Watkins and Gooray [3] have all recently reviewed the literature in this area. Most of the experiments cited in the reviews contained only mean heat transfer rates and very little fluid dynamic data. The data sets show the same general features for a variety of geometries: a drop in the heat transfer coefficient at separation followed by a sharp rise in the reattachment zone.

Aung and Goldstein [10] used a Mach-Zehnder interferometer to measure temperature profiles and heat transfer coefficients in the back-step geometry. There was a significant temperature gradient across the free shear layer just downstream of separation, but they concluded that the heat transfer resistance is concentrated in the near-wall region for most of the flow.

Generally, it has been assumed that the point of maximum heat transfer coefficient corresponds to the mean reattachment point. However, Kang et al. [11] and Suzuki et al. [12] contradicted this assumption after a series of experiments on confined coaxial jets. They measured the Nusselt number using a constant heat-flux surface and collected mean-velocity and turbulence data with a laser-doppler anemometer. They showed clearly that the peak heat transfer coefficient occurs well upstream of reattachment. They also showed that the Nusselt number correlates well with the turbulence intensity measured at $y = 4$ mm, their point nearest to the wall.

Armaly et al. [13] presented heat transfer, mass-transfer, and fluid-dynamic data for a sudden expansion at relatively low Reynolds numbers. The peak in the Sherwood number was clearly upstream of reattachment for turbulent flows, but both the Sherwood and Nusselt number data showed a double peak for laminar flows. Heat transfer data were not presented for the higher Reynolds numbers.

Recently Chieng and Launder [14] applied the k–ϵ model of turbulence to the prediction of separated-flow heat transfer. Their model assumes that the length scale in the near-wall region depends only on the normal distance from the wall and that the viscous sublayer thickness adjusts itself as a specified function of the external turbulence energy. No separated-flow data are available to check these assumptions, and recent experiments reported by Simpson et al. [15], Eaton and Johnston [4], and Westphal et al. [7] suggest that the near-wall region of separated flow is substantially different from the corresponding region in an ordinary boundary layer.

The objective of the present experiment was to provide detailed heat transfer data coupled with temperature and velocity profiles. These data will provide a well-documented test case and physical insight into the mechanisms controlling the heat transfer rate in reattaching flows. The emphasis is placed on the near-wall region, which controls the heat transfer rate.

The measurements presented here are a subset of data presented in a full report (Vogel and Eaton [16]). Some of the fluid-dynamic measurements are drawn from the report of Adams et al. [17].

[1]Present address: Contour Medical Systems, Mountain View, CA

Contributed by the Heat Transfer Division for publication in the JOURNAL OF HEAT TRANSFER. Manuscript received by the Heat Transfer Division January 19, 1984. Paper No. 83-WA/HT-11.

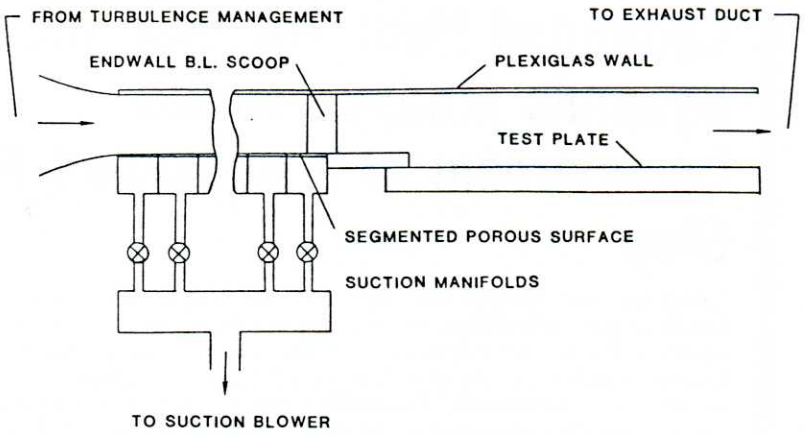

Fig. 1 Test section schematic

Experimental Apparatus

The facility (see Fig. 1) is an open-circuit, two-dimensional, sudden-expansion wind tunnel. It consists of a blower and turbulence management section, a boundary-layer development section, and a sudden-expansion test section.

After the air is filtered upstream of the blower, mineral-oil smoke (particle size 1/2 μ) is added to provide seeding for the laser-doppler anemometry. The flow is provided by an airfoil-bladed blower driven by a computer-controlled AC motor. Turbulence management consists of a honeycomb, four screens, and a 4:1 two-dimensional contraction. The free-stream turbulence level in the test section is less than 0.2 percent, and total pressure nonuniformity as documented by spanwise traverses was less than 1 percent.

The test boundary layer develops on the bottom surface of the 15 cm × 51 cm development section, which is 2.5 m long. The bottom wall is porous, and transpiration may be used to vary the boundary-layer thickness at the test-section entrance from 0.3 to 6 cm.

The sidewall boundary layers are removed by scoops upstream of the test section to reduce the strength of any secondary flows. The scoops narrow the test section to a width of 45 cm. After the scoops, there is a 0.2-m-long flat section before the boundary layer flows over the 3.8-cm-high backward-facing step (expansion ratio = 1.25).

Mass and momentum balances were performed on the test section using pitot-tube profiles at the inlet reference station and exit plane and skin-friction measurements on both the top and bottom walls of the tunnel. Both balanced within 3 percent of the inlet flux, indicating that the flow is two dimensional within the uncertainty of the measurements.

Two test surfaces were used, one a clear Plexiglas plate with

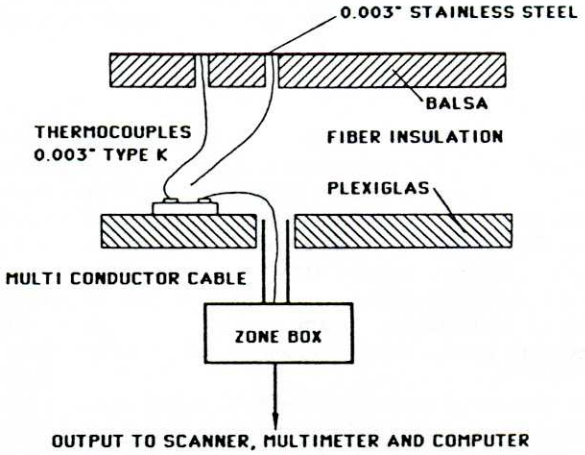

Fig. 2 Cross section of the heat transfer measurement surface

instrument ports for near-wall measurements. The thermal tuft and pulsed-wall probe are mounted in this surface for obtaining forward-flow fraction and skin-friction data, respectively. The other is a constant-heat-flux heat transfer measurement surface. The two are easily interchanged.

The heat transfer measurement plate consists of a thin (0.003 in.), stainless steel foil glued smoothly to a balsa-wood backing (Fig. 2). Forty type-K, 0.003-in.-dia thermocouples are welded to the back surface, for temperature measurement. The thermocouples were placed in grooves cut in the balsa parallel to the surface. Conduction along the fine thermocouples was therefore negligible. Alternating current is supplied to the busbars through a large stepdown transformer, to provide a constant heat flux from the surface.

Nomenclature

AR = area ratio, upstream height/downstream height

C_f = instantaneous skin-friction coefficient $= \tau_0 \Big/ \frac{1}{2}\rho_\infty U_{ref}^2$

$\bar{C}_f$ = time mean skin-friction coefficient

C_f' = fluctuating component of C_f

c_∞ = free-stream specific heat

h = heat transfer coefficient = $\dot{q}_0''/(T_w - T_\infty)$

H = step height

$\dot{q}_0''$ = wall heat transfer rate per unit area

Re_H = step-height Reynolds number $= U_{ref}H/\nu$

St = Stanton number = $h/U_{ref}\rho_\infty c_\infty$

$\bar{T}$ = local mean temperature

T_∞ = free-stream temperature

T_w = local wall temperature

$\bar{U}$ = mean streamwise velocity

u' = fluctuating component of streamwise velocity

u^+ = nondimensional velocity = $U/\sqrt{\tau_0/\rho}$

U_{ref} = reference free-stream velocity measured at $x/H = -3$

x = streamwise coordinate measured from step edge

x_R = reattachment length

y = coordinate normal to wall

y^+ = nondimensional distance from wall = $y\sqrt{\tau_w/\rho}/\nu$

γ = forward-flow fraction

ν = freestream kinematic viscosity

ρ_∞ = freestream density

τ_0 = local wall shear stress

Conduction through the back insulation accounts for less than 1 percent of the total heat transfer from the foil, while conduction along the surface accounts for a smaller fraction, even in regions of high temperature gradient. At these current densities in the surface, the Hall effect can be expected to introduce approximately a 1 percent uncertainty in the centerline heat-flux measurements (Tarasuk and Castle [18]). The heat flux from the surface is uniform within this limitation, and the heat transfer coefficient can be determined simply by measuring the difference between the surface and free-stream temperatures.

The heat transfer surface was qualified by lifting it into position flush with the upstream boundary-layer development section thereby providing an unheated starting-length flat plate. The deviation between the data and flat-plate correlations was less than 2 percent. Four spanwise rows of thermocouples were placed in the surface to check on the two dimensionality of the heat transfer data. For all measurements, the scatter in the spanwise direction was less than 5 percent about the mean.

Mean temperature profiles are measured using a traversing thin-wire thermocouple probe. This probe is similar in appearance to a hot-wire probe but has an 0.003-in.-dia butt-welded thermocouple junction at the center of the wire with an aspect ratio of 100:1.

A pulsed wall probe was used to measure the time-averaged and fluctuating skin friction. This probe, which is described in detail in Eaton et al. [6], is capable of measuring the velocity very near the wall in highly unsteady flow. Eaton et al. [6] and Westphal et al. [7] have demonstrated that the probe can be used to accurately measure the skin friction when the wires are placed in the viscous sublayer. In practice, the wires were set to a fixed height (0.13 mm) and the probe was calibrated in a laminar channel flow of known skin friction.

The thermal tuft (Eaton et al. [6]) measures the instantaneous sign of the velocity at a height of about 1 mm above the surface. At a given location the fraction of time that the flow is in the downstream direction is measured. Eaton et al. [6] showed that the point of 50 percent forward-flow fraction corresponds to the mean reattachment point ($C_f = 0$) with an uncertainty of less than 0.1 step heights.

Velocity measurements are made in the flow using a single-component, forward-scattering LDA system. A 2-W, argon-ion laser is used with T.S.I. optics and a counter type processor. A beam expander was used to give a large beam intersection angle of 15 deg. A number of different sampling schemes were used to ensure minimal velocity bias (see Adams et al. [19]). Generally, direct time averaging proved very satisfactory.

Results

This paper presents the detailed heat transfer and relevant fluid-dynamic data for the investigation of the near-wall region. Complete details of the flow measurements, including velocity and turbulent transport, are contained in Adams et al. [17] and Vogel and Eaton [16]. The reference free-stream velocity for the measurements presented here is 11.3 m/s, which corresponds to a step-height Reynolds number of 28,000. The expansion ratio is held constant at 1.25, and the aspect ratio of the tunnel is 12. The heat flux through the heat transfer surface is 270 W/m^2, corresponding to a maximum temperature of 15°C above ambient. A low-overheat ratio was used to minimize variable-properties effects. Table 1 presents estimates of the errors for each of the measurands. The uncertainty in most of the measurands was calculated by estimating the calibration and reading uncertainties for each instrument. The component uncertainties were then combined using the method of Kline and McClintock [20]. The un-

Table 1 Uncertainties

St	0.00025
C_f	0.0002
C_f'	0.00015
$\dot{q}_0''$	2 W
u^+	1
$T - T_{inf}$	0.1°C
U/U_{ref}	0.01
u'/U_{ref}	0.02

Table 2 Parameters describing inlet boundary layer for reference case

Reference conditions:	$U_{ref} = 11.3$ m/s
	$Re_H = 28{,}000$
Boundary-layer parameters (measured at $x/H = -3.8$)	
Boundary-layer thickness	$\delta_{99} = 4.05$ cm
Momentum thickness	$\theta = 0.468$ cm
Momentum-thickness Reynolds number	$Re_\theta = 3370$
Shape factor	$H = 1.389$
Skin friction (log-law fit)	$C_f = 0.00312$

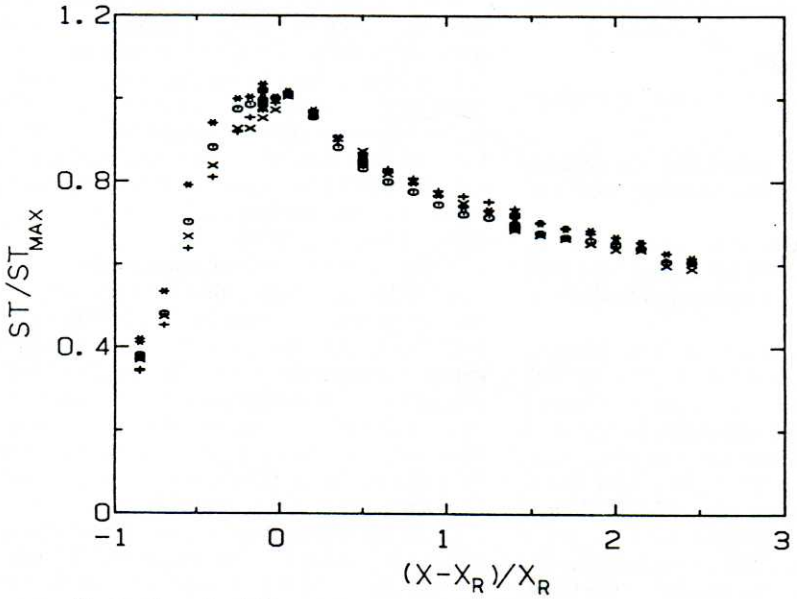

Fig. 3 Normalized Stanton number profiles for δ/h = 1.1: • Re_H = 13,000; ○ Re_H = 20,000; × Re_H = 28.000; + Re_H = 42,000

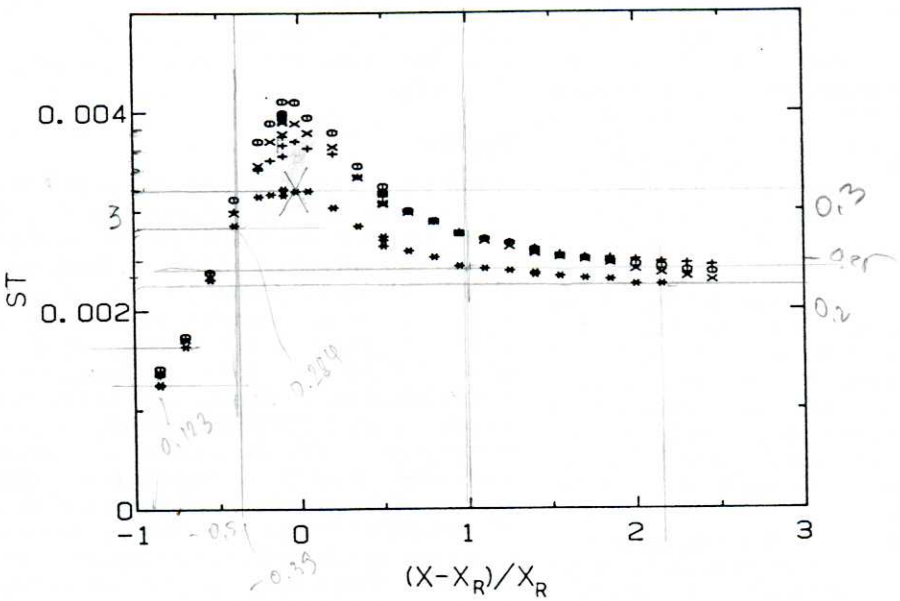

Fig. 4 Stanton number profiles with varying upstream boundary-layer thickness at a Reynolds number of 28,000: ○ δ/h = 0.15; × δ/h = 0.19; + δ/h = 0.7; * δ/h = 1.1

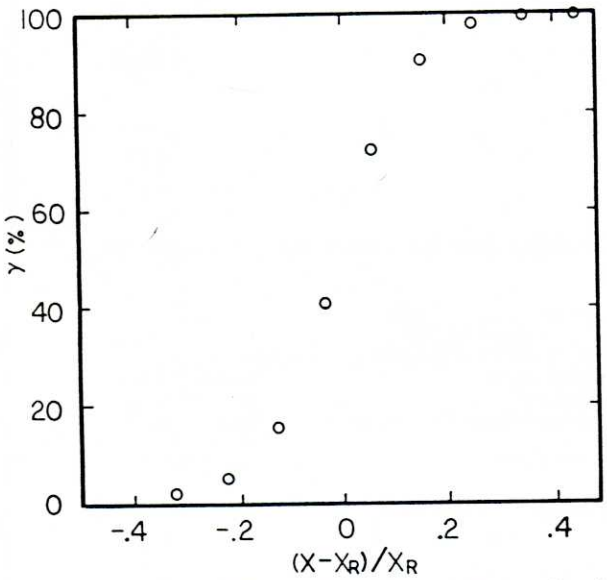

Fig. 5 Profiles of γ (fraction of time flow is in downstream direction) for reference case

certainties in the LDA data were calculated statistically, because the calibration and reading uncertainties were virtually zero.

The inlet velocity profile was measured at a station 3.8 step heights upstream of the step. The profile agreed well with conventional log-law plots. Profile parameters are tabulated in Table 2.

Stanton-number profiles were obtained at four different step-height Reynolds numbers ranging from 13,000 to 42,000. These data are presented in Fig. 3 in terms of the Stanton number normalized on the maximum value plotted against a nondimensional streamwise coordinate ($x^* = (x - x_R)/x_R$), where x_R is the reattachment length. This nondimensionalization has been shown by Westphal and Johnston [21] to collapse the fluid-dynamic data for single backward-facing steps. In the present experiments, the reattachment point is located 6-2/3 step heights downstream of separation.

All the Stanton-number profiles show the same general features. There is a low heat transfer rate in the recirculation region, followed by a steep rise to the maximum near the reattachment point. Previous work showed the maximum heat transfer point anywhere from three to five step heights from the backstep. The peak heat transfer rate in the present experiment occurs slightly upstream of reattachment, as measured by the thermal tuft. The apparent maximum is on the order of 0.1 reattachment lengths (x^*) upstream of mean reattachment, corresponding to 2/3 of a step height for this flow. The actual peak Stanton number varies inversely with the Reynolds number (see below).

Downstream of reattachment, the Stanton number recovers toward that found under a normal turbulent boundary layer. The recovering boundary layer behaves much like a boundary layer with an unheated starting length upstream of the heated section. The effective origin of the redeveloping thermal boundary layer lies approximately two step heights downstream of reattachment for all Reynolds numbers.

In Fig. 4, the dependence of the Stanton number profile on boundary-layer thickness at separation is shown. The upstream boundary layer is turbulent in all cases presented here. It is apparent that the upstream shear layer thickness has a significant effect near reattachment but very little effect either up or downstream of reattachment. Figure 5 shows the forward-flow fraction as measured with the thermal tuft. The region of reversing flow corresponds roughly to the region where the upstream boundary-layer thickness has a significant effect on the Stanton number.

In Fig. 6, the maximum Stanton number is plotted for each value of boundary-layer thickness and Reynolds number. The maximum was measured by hand from the Stanton-number profiles. For all boundary layers and Reynolds numbers, the curves are smooth and monotonic in shape. This behavior suggests that a correlation for the maximum heat transfer rate as a function of these two parameters would be possible. However, such a correlation would obscure the different behavior of the profiles when the two parameters are varied independently (see Figs. 3 and 4).

Mean velocity and streamwise turbulence intensity profiles for the reference case are presented in Figs. 7 and 8. These profiles show the typical features that have been observed in other backward-facing step experiments. It is noteworthy that the peak value of the turbulence intensity occurs slightly

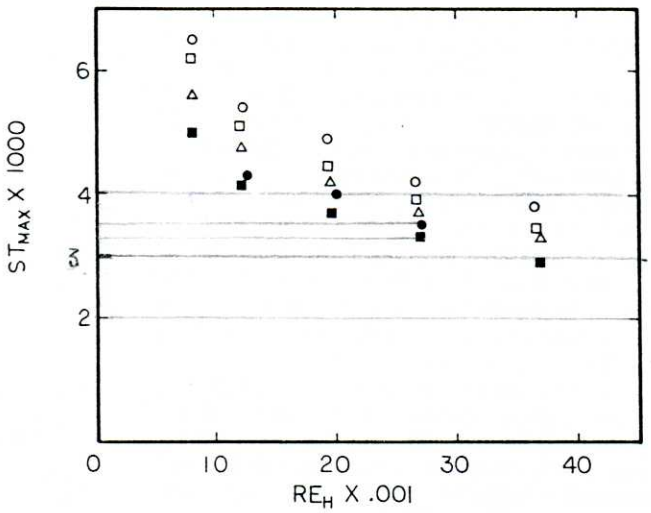

Fig. 6 Peak Stanton number as a function of Reynolds number and upstream boundary-layer thickness: ○ δ/h = 0.15; □ δ/h = 0.19; △ δ/h = 0.7; ● δ/h = 1.1; ■ δ/h = 1.6

upstream of the mean reattachment point near the location of the peak Stanton number.

Eight temperature profiles (Fig. 9) were taken at various distances downstream of the backstep using the thermocouple probe. These compare very well with the results of Aung and Goldstein [10], obtained using interferometry. As can be seen from these profiles, most of the thermal resistance is in the region very close to the wall, which is conduction dominated. In only one of the profiles, that closest to the step, is there a considerable temperature gradient in the flow far from the wall. Convective mixing effects everywhere else are great enough to flatten any temperature gradients. The near-step recirculation-region velocities are very small compared to the free-stream, producing more nearly stagnant air.

The temperature profiles show that the heat transfer resistance is dominated by the near-wall region. Clearly the fluid mechanics of the near wall region must be very important in determining the local Stanton number. The behavior of the near-wall flow is most simply quantified by the mean and fluctuating skin friction. In Fig. 10, the mean skin friction coefficient ($\bar{C}_f$) along the lower wall is plotted for the reference inlet conditions. The skin friction follows the

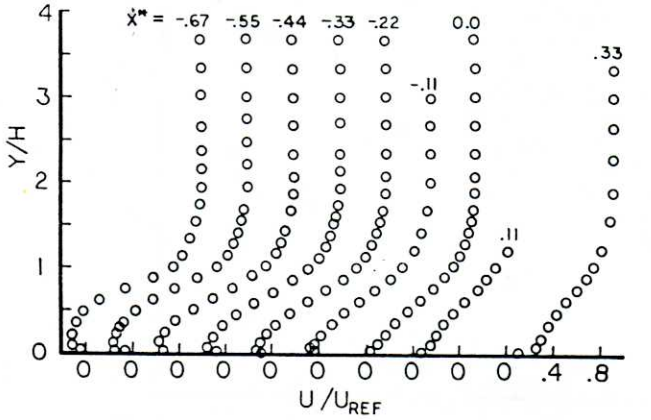

Fig. 7 Mean velocity profiles for reference conditions; most of points near the wall omitted for clarity

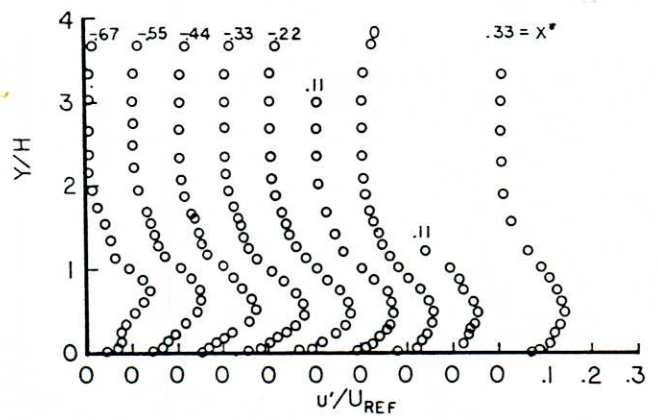

Fig. 8 Streamwise turbulence intensity (u') profiles for reference conditions; most of points near the wall omitted for clarity

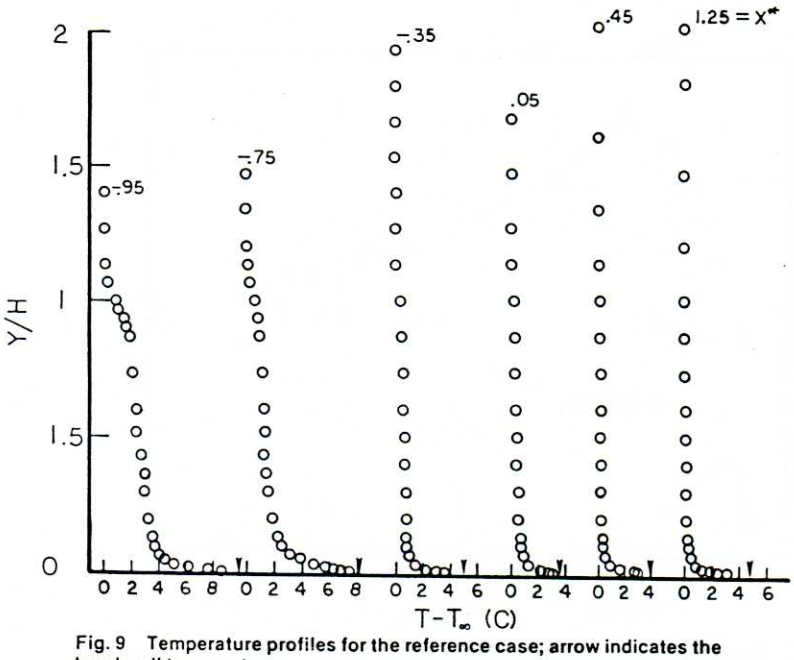

Fig. 9 Temperature profiles for the reference case; arrow indicates the local wall temperature

al behavior for backstep flow. It is negative in the kflow region of recirculation, passes through zero at ttachment, and then increases downstream. The skin-tion coefficient is slightly positive close to the step edge, icating the corner eddy. In the recirculation region, the ative skin friction is fairly large, about 50 percent of the -downstream value.

The fluctuating component of the skin friction is shown in . 11 for the reference Reynolds number and two different ndary-layer thicknesses. Near the backstep, the velocities low and the flow is not very turbulent. Moving toward ttachment, the flow is very unsteady close to the wall, with maximum fluctuations in the vicinity of reattachment. e maximum fluctuating component of the skin friction is re than 40 percent of the maximum mean skin friction. th profiles then relax toward a far-downstream value. The ctuating skin-friction variation with boundary-layer ckness is discussed in the next section.

scussion

The peak in the Stanton number around reattachment varies as the -0.4 power of the Reynolds number, while the flat-plate flow Stanton number varies as the -0.2 power of Reynolds number. The exponent for the reattaching flow is similar to that of experiments on impinging jet flows, which show Stanton-number dependence on Reynolds number of -0.42 for a wide range of impingement angles (Kumada et al. [22]). The fairly good collapse of these profiles suggests that the Stanton number scales everywhere on Reynolds number.

In contrast, the Stanton-number profiles changing with the initial thickness of the separated shear layer do not collapse to a single profile when normalized on the maximum value. The Stanton number is nearly independent of boundary-layer thickness in the recirculating flow region and redeveloping boundary layer but varies significantly within the reattachment region. The change in the reattachment length was small for the same thickness variation so the mean flow is probably not substantially changed. The variation in the Stanton number with boundary-layer thickness must therefore be attributed to variations in the turbulent structure.

The question remains: What controls the heat transfer

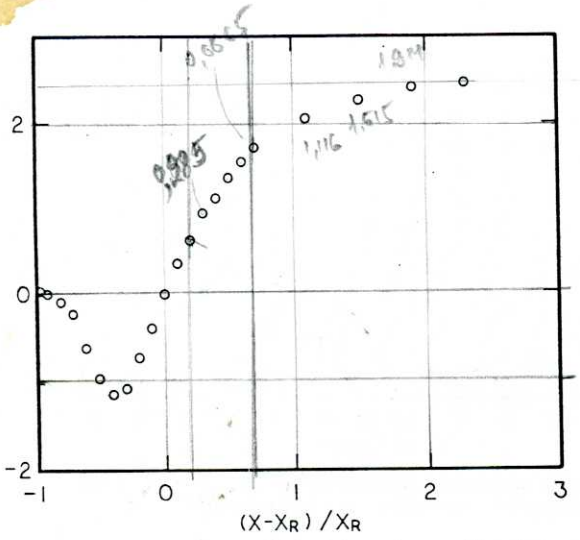

Fig. 10 Mean skin-friction coefficient downstream of the step

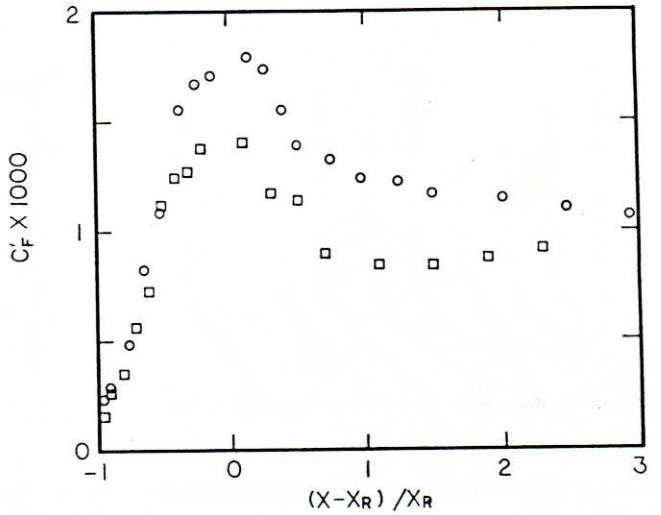

Fig. 11 RMS skin-friction fluctuations for a Reynolds number of 28,000: ○ $\delta/h = 0.15$; □ $\delta/h = 1.1$

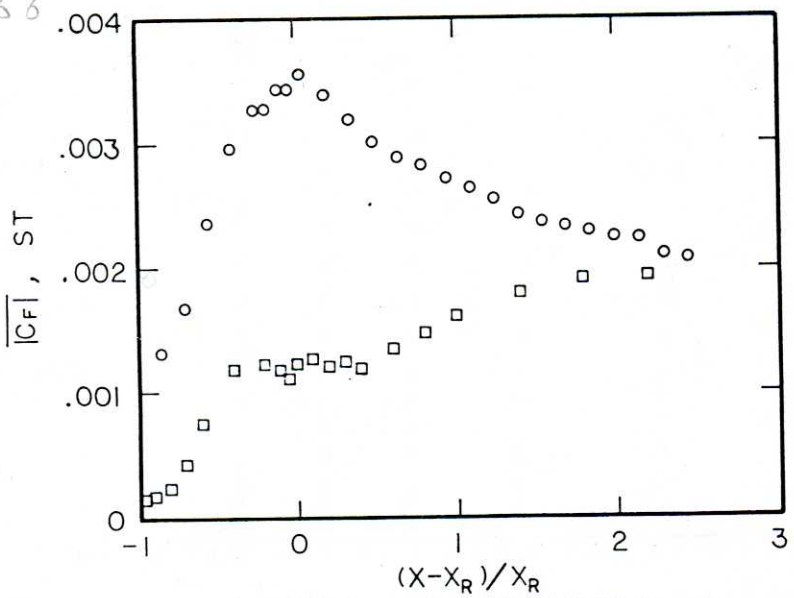

Fig. 12 Comparison of Stanton number and time average of the absolute value of the skin friction for the reference case: ○ St; □ $\overline{|C_f|}$

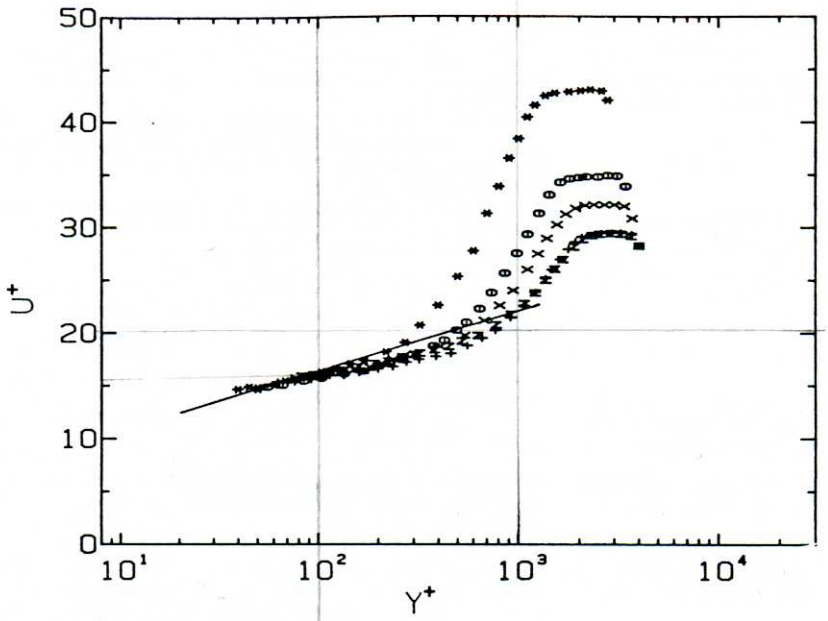

Fig. 13 Mean velocity downstream of reattachment for the reference case: * $x/H = 10$; ○ $x/H = 12$; × $x/H = 14$; z $x/H = 16$; + $x/H = 18$

coefficient in the reattachment zone? Obviously, the Stanton number is not determined by the mean flow. The Reynolds analogy fails entirely, since the skin friction passes through zero near the point of maximum Stanton number. It has been suggested that the Reynolds analogy may apply instantaneously in reattaching flows. If that is the case, one would expect the Stanton number to be related to the time average of the absolute value of the skin friction ($\overline{|C_f|}$). This quantity is estimated from the measured mean and fluctuating skin friction by assuming a Gaussian probability distribution for the skin friction. Eaton and Johnston [4] have shown that the probability distribution can be reasonably approximated by a Gaussian distribution near reattachment.

Figure 12 shows the time average of the absolute value of the skin friction and the Stanton-number profile. The agreement between the two curves is poor except well downstream of reattachment, where the thermal boundary layer behaves like that on a flat plate. Downstream of the reattachment zone there are no flow reversals and $\overline{|C_f|}$ is just equal to the mean skin friction. Therefore the data show that the Reynolds analogy does hold in the recovering boundary layer.

The Stanton number can be related to the thickness of the thermal (or hydrodynamic) sublayer. The sublayer is very thin in the reattachment region corresponding to the high Stanton number. The region of high temperature gradient is two to three times thicker in the recirculation region corresponding to the lower Stanton number. Adams, Johnston, and Eaton [17] have shown that the near-wall layer below the recirculating flow grows as a laminar boundary layer for the moderate Reynolds number of this experiment. Such laminar boundary layer growth corresponds to a decrease in the Stanton number moving away from reattachment. Downstream of reattachment the sublayer grows as it would under an unheated starting-length boundary layer. Again, the thickening of the sublayer accounts for the reduction in the Stanton number.

Within the reattachment zone, the Stanton number is apparently controlled by the turbulence level near the wall. The fluctuating skin friction is much higher than under an ordinary boundary layer, because very energetic free-shear-layer eddies are impinging on the wall. The RMS level of the skin-friction fluctuations is determined by the structure of the impinging shear layer. When the upstream layer is thin, the shear-layer turbulence is more energetic and the skin-friction fluctuations are large relative to a thick boundary layer case. The larger skin-friction fluctuations result in a proportionally larger Stanton number.

It is frequently observed that the recovering boundary layer remains disturbed for a long distance downstream of reattachment (cf. Bradshaw and Wong [23]). This observation seems in conflict with the fact that the Stanton number returns quickly to a flat-plate profile. Log plots of the mean-velocity profiles downstream of reattachment (Fig. 13) show that the disturbance in the boundary layer is primarily in the outer part of the log region. The inner part of the boundary layer which controls the heat-transfer resistance is largely undisturbed.

Summary and Conclusions

The present heat transfer measurements are in general agreement with previous experiments; reattachment causes a local augmentation of the heat transfer coefficient by a factor of about two. The maximum heat transfer coefficient occurs slightly upstream of reattachment, where the peak values of the turbulence intensity are measured. The heat transfer coefficient recovers fairly rapidly to flat-plate behavior downstream of reattachment.

As in other turbulent flows the majority of the heat transfer resistance occurs in the near-wall region. Turbulent mixing in the separated free-shear layer is very strong except close to the step. Downstream of $x/h = 2$, there is virtually no temperature gradient across the separated shear layer. The large temperature gradients in the near-wall region point out the importance of understanding this zone if the heat transfer is to be predicted accurately.

In the various regions of the flow, different physical mechanisms act to control the heat transfer coefficient. For example, moving upstream from reattachment, the near-wall layer grows as a laminar boundary layer, thickening as it approaches the center of the recirculation bubble. The thickening of this layer causes the heat transfer coefficient to drop rapidly. Well downstream of reattachment, the near-wall layer behaves like that under an ordinary turbulent boundary layer. The heat transfer coefficient is determined by the local skin friction, and the Reynolds analogy applies.

Within the reattachment region there is essentially no mean

n the near-wall region and the effective conductivity of ar wall zone is determined by the intensity of turbulence ations. Variations in the Stanton number correlate well ariations in the rms level of skin friction fluctuations.

iowledgments

thank the Heat Transfer Program of the National ce Foundation for supporting this work (Grant #MEA-89). Dr. Win Aung is the responsible program manager.

rences

aton, J. K., "Summary of Computations for Cases 0421, 0431, P2, and eparated Internal Flows," *Proceedings 1980=81 AFOSR-HTTM-rd Conference on Complex Turbulent Flows:* Vol. III, *Comparison of itation and Experiment*, 1982.

aton, J. K., and Johnston, J. P., "A Review of Research on Subsonic lent Flow Reattachment," *AIAA J.*, Vol. 19, No. 9, Sept. 1981, pp. 100.

Watkins, C. M., and Gooray, A. M., "Numerical Calculations of Tur- Recirculating Heat Transfer Beyond Two-Dimensional Backsteps and n Pipe Expansions," Dept. of Mech. Engrg., Howard University, ngton, D.C., Aug. 1982.

Eaton, J. K., and Johnston, J. P., "Turbulent Flow Reattachment: An mental Study of the Flow and Structure Behind a Backward-Facing Rept. MD-39, Dept. of Mech. Engrg., Stanford University, June 1980.

Durst, R., and Tropea, C., "Turbulent, Backward-Facing Step Flows in Dimensional Ducts and Channels," *Proceedings of the 3rd International sium on Turbulent Shear Flows*, Davis, CA, 1981.

Eaton, J. K., Westphal, R. V., and Johnston, J. P., "Two New In-nts for Flow-Direction and Skin-Friction Measurements in Separated ," *ISA Transactions*, Vol. 21, No. 1, 1982, pp. 69-78.

Westphal, R. V., Eaton, J. K., and Johnston, J. P., "A New Probe for irement of Velocity and Wall Shear Stress in Unsteady, Reversing Flow," *ids Engrg.*, Vol. 102, No. 2, 1981, pp. 478-482.

Fletcher, L. S., Briggs, D. G., and Page, R. H., "Heat Transfer in ated and Reattaching Flows: An Annotated Review," *Israel J. of Tech.*, 12, 1974, pp. 236-261.

Aung, W., and Watkins, C. B., "Heat Transfer Mechanisms in Separated d Convection," *Proceedings of the NATO Institute on Turbulent Forced Convection in Channels and Bundles: Theory and Applications to Heat Exchangers*, Turkey, June 20-Aug. 2, 1978.

10 Aung, W., and Goldstein, R. J., "Heat Transfer in Turbulent Separated Flow Downstream of a Rearward-Facing Step," *Israel J. of Tech.*, Vol. 10, 1972, pp. 35-41.

11 Kang, Y., Nishino, J., Suzuki, K., and Sato, T., "Application of Flow Surface-Temperature Visualization Techniques to a Study of Heat Transfer in Recirculating Flow Regions," *Flow Visualization II*, ed. W. Merzkirch, Hemisphere, 1982, pp. 77-81.

12 Suzuki, K., Ida, S., and Sato, T., "Turbulence Measurements Related to Heat Transfer in an Axisymmetric Confined Jet with Laser-Doppler Anemometer," *Proceedings of 4th Symposium on Turbulent Shear Flows*, Karlsruhe, Germany, Sept. 1983, pp. 18.1-18.6.

13 Armaly, B. F., Durst, F., and Kottke, V., "Momentum, Heat and Mass Transfer in Backward-Facing Step Flows," *Proceedings of 3rd Symposium on Turbulent Shear Flows*, Davis, CA, Sept. 1981, pp. 16.1-16.4.

14 Chieng, C. C., and Launder, B. E., "On the Calculation of Turbulent Heat Transport Downstream From an Abrupt Pipe Expansion," *Numerical Heat Transfer*, Vol. 3, 1980, pp. 189-207.

15 Simpson, R. L., "A Model for the Backflow Mean Velocity Profile," *AIAA J.*, Vol. 21, No. 1, 1983, pp. 142-143.

16 Vogel, J. C., and Eaton, J. K., "Heat Transfer and Fluid-Mechanics Measurements in the Turbulent Reattaching Flow Behind a Backward-Facing Step," Report MD-44, Thermosciences Division, Dept. of Mech. Engrg., Stanford University, July 1984.

17 Adams, E. W., Johnston, J. P., and Eaton, J. K., "Experiments on the Structure of Turbulent Reattaching Flow," Report MD-43, Thermosciences Division, Dept. of Mech. Engrg., Stanford University, May 1984.

18 Tarasuk, J. D., and Castle, G. S. P., "Temperature Distribution in an Electrically Heated, Wide, Metallic Foil," ASME JOURNAL OF HEAT TRANSFER, Vol. 105, Feb., 1983, pp. 210-212.

19 Adams, E. W., Eaton, J. K., and Johnston, J. P., "An Examination of Velocity Bias in a Highly Turbulent Separated and Reattaching Flow," *Proceedings of the 2nd Int'l. Symposium on Applications of Laser Anemometry to Fluid Mechanics*, Lisbon, Portugal, July 1984.

20 Kline, S. J., and McClintock, F. A., "Analysis of Uncertainty in Single-Sample Experiments," *Mechanical Engineering*, Jan. 1952.

21 Westphal, R. V., and Johnston, J. P., "Effect of Initial Conditions on Turbulent Reattachment Downstream of a Backward-Facing Step," *AIAA J.*, Vol. 22, No. 12, 1984, pp. 1727-1732.

22 Kumada, M., Mabuchi, I., and Oyakawa, K., "General Correlation of Mass Transfer by Reattached Jet at Stagnation Point on a Plate," *Heat Transfer – Japanese Research*, Vol. 3, Jan. 1974, pp. 93-103.

23 Bradshaw, P., and Wong, F. Y. F., "The Reattachment and Relaxation of a Turbulent Shear Layer," *J. Fluid Mechanics*, Vol. 152, Part 1, 1972, pp. 113-135.